



Acknowledgements:

National Science Foundation
WHERE DISCOVERIES BEGIN



Biopolymers as carriers of natural (Th, Pa, Pb, Po, Be) and waste (e.g., Pu, I) radionuclides in aquatic systems



Peter H. Santschi
Texas A&M University
Galveston, TX, 77553, USA



Objectives

- Relate environmental chemistry of Be to that of other radionuclides.
- Explore role of biopolymeric carriers for radionuclides in the environment.
- Lessons from field and lab studies using ‘correlative’ and ‘extractive’ approach.
- Relevance for remediation, interpretation of results from applications, e.g., historical reconstructions, etc.

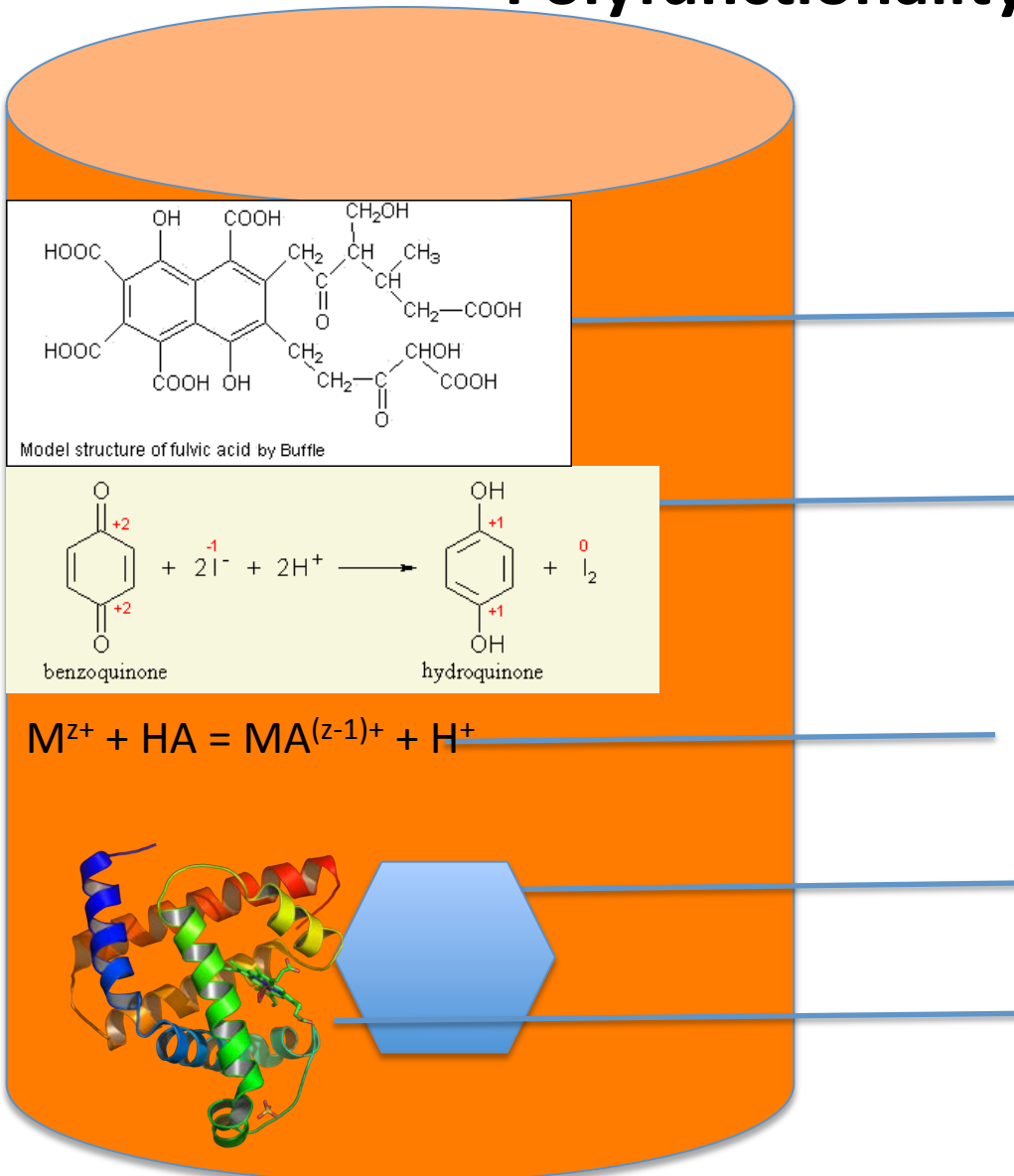
Common Uses of Natural Radionuclides in Environment: Cosmic Ray Produced and Parent-Daughter Radionuclide Pairs allow

- Tracing particle-associated pathways, fluxes, and residence times in ocean and lakes
- Tracing of different water masses in ocean
- Tracing diffusion/advection in ocean and lakes
- Paleo-reconstruction of climate, ocean mixing, nutrient and pollutant levels, etc.

Common (multiple) oxidation states of environmental radionuclides

- A-type: U(IV,VI), Th(IV), Pa(IV,V), Pu(III,IV,V), Be (II)
- B-type: Pb(II, IV)
- Metalloid: Po(-II, II, IV), I(-I, 0, I, V)

Biomolecules as Carriers of Radionuclides due to their Polyfunctionality



Chelating Site:
Ligand exchange

Electron-(redox) active Site:
Electron exchange, radical
Formation

Anionic Site:
Proton exchange

Chemical Reaction Site:
example aromatic C for I

Hydrophobic Reaction Site:
pI, pH and pE dependent
folding resulting in 3-dim.
structure

Evidence for organic carriers for different colloidal radionuclides

- ‘Extractive’ Approach: Composition of isolated colloids (e.g., Pu, Th, I)
- ‘Correlative’ Approach: Relationships between DOC/PS/APS and colloidal radionuclide concentrations (e.g., Th)
- ‘Correlative’ Approach: Relationships between POC/ ^{234}Th or Pa/Th ratios in particles and compositional parameters such as acid polysaccharide (APS) concentrations (e.g., Th, Pa)
- ‘Correlative’ Approach: Relationships between aromatic C and I in colloids

Reasons for Study

- Why do we want to know this?
- -> Remediation , interpretation of results, forecasting, allows decision in controversies
- Requires overarching approaches crossing established disciplines, but limited by “Environmental Heisenberg uncertainty principle”
- High reward, as it might cause a Paradigm shift, but full of potential artifacts.
- Architecture of environmental macromolecules: inside hydrophobic, outside hydrophilic, with chelating and redox active sites → ‘All-in-one’ carrier bio-geo-polymers?

Evidence

from

Correlations

But:

SiO₂ is

Weak

sorbent

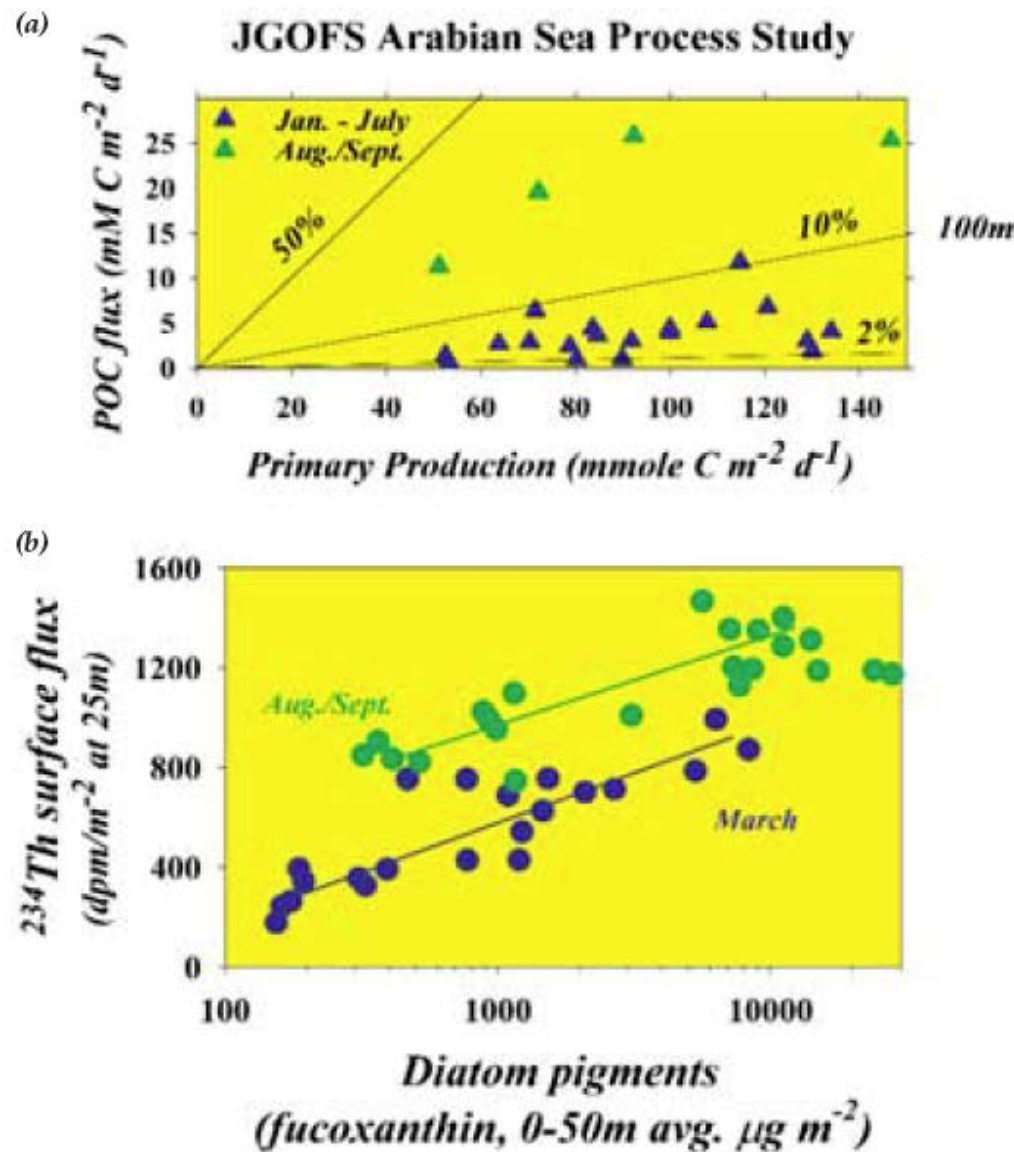


Figure 5. a) Relationship between primary production and Particulate Organic Carbon (POC) export derived from ^{234}Th measurements at 100 m in the Arabian Sea. Note high ratio of POC flux to primary production in August and September. b) Relationship between ^{234}Th export and fucoxanthin (diatom) pigments, showing higher ratio of ^{234}Th export to fucoxanthin flux in August and September during the latter part of the southwest monsoon.

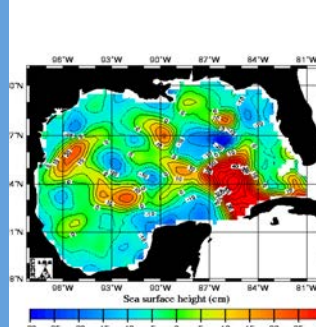
Relationship between $^{234}\text{Th}/\text{POC}$ ratio and POC-normalized APS and Carbohydrate Concentrations [Guo et al., 2002, Mar. Chem. 78, 103-119; Santschi et al., GRL.30,C2, 1044]

2001 cruise to Gulf of Mexico:

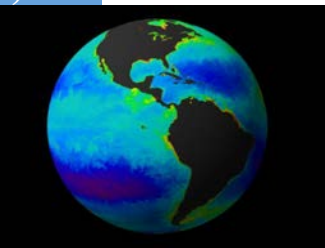
Filled circles: sinking particles

Collected at 65, 90, 120 m depth; Open circles:

suspended particles (sum of 0.5, 1, 10, 53 μm fractions)

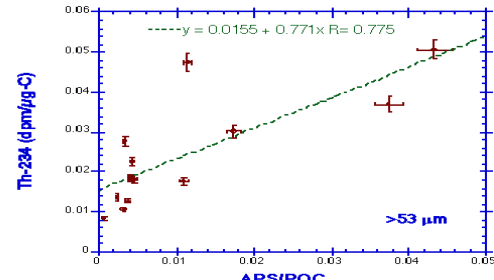
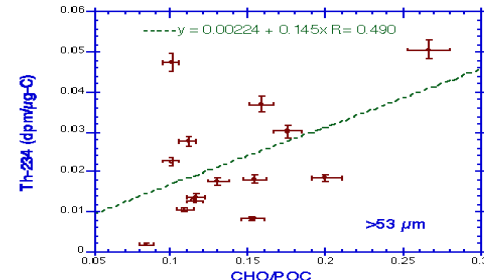
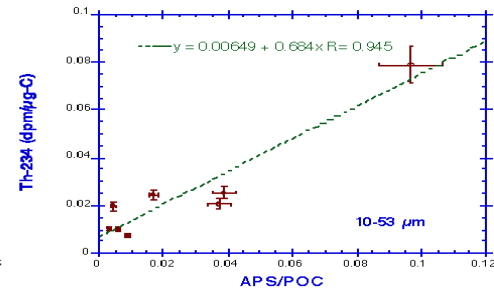
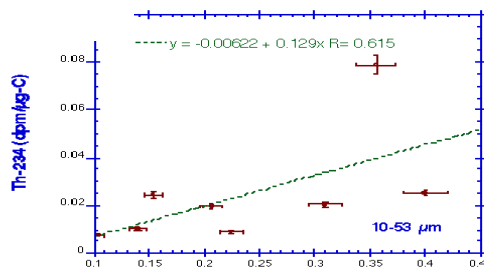
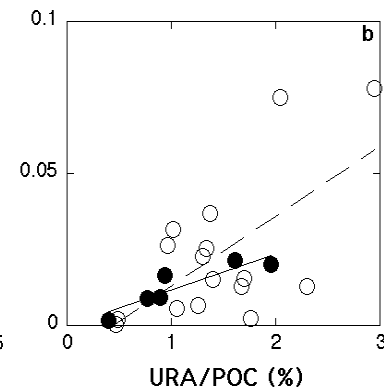
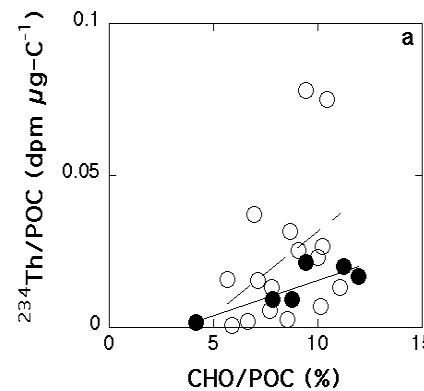


- CHO /OC~0.1
- URA,APS/OC~0.01

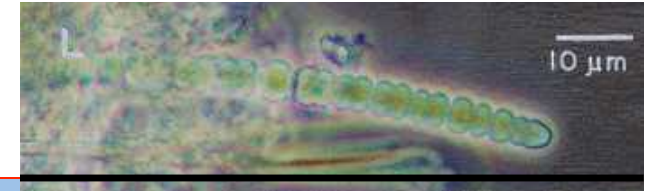


Lig./POC ~ 0.001 (Hirose, 2004); $^{234}\text{Th}/\text{Lig.} \sim 10^{-7} - 10^{-12}$

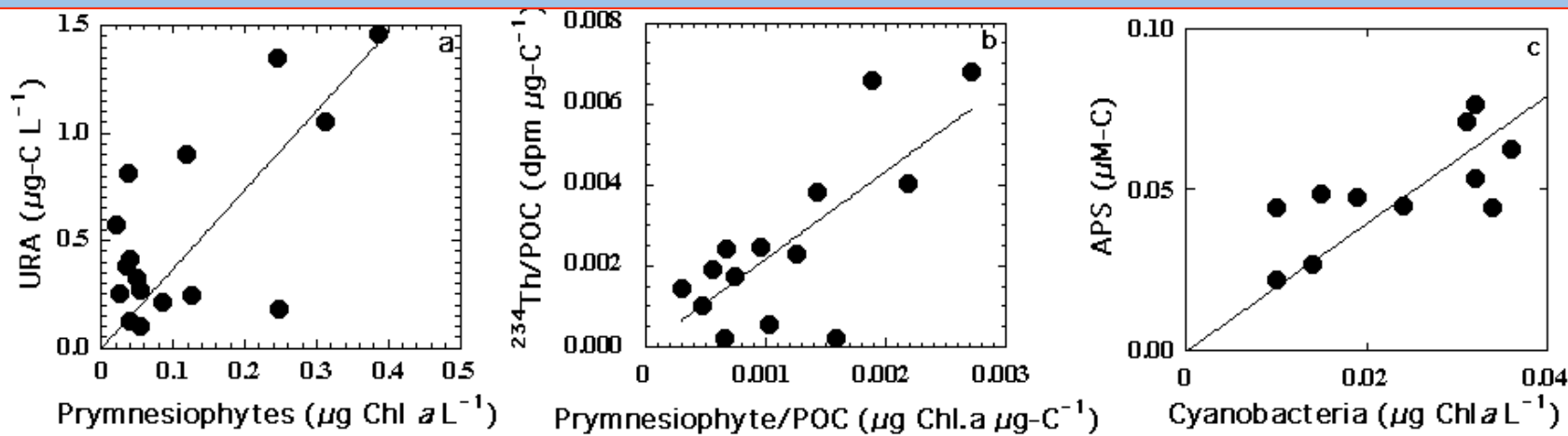
2000 cruise to Gulf of Mexico: Open circles: suspended particles



Importance of **Prymnesiophytes** in 2001 and Cyanobacteria in 2000 [Santschi et al., 2003, GRL 30, 1044]

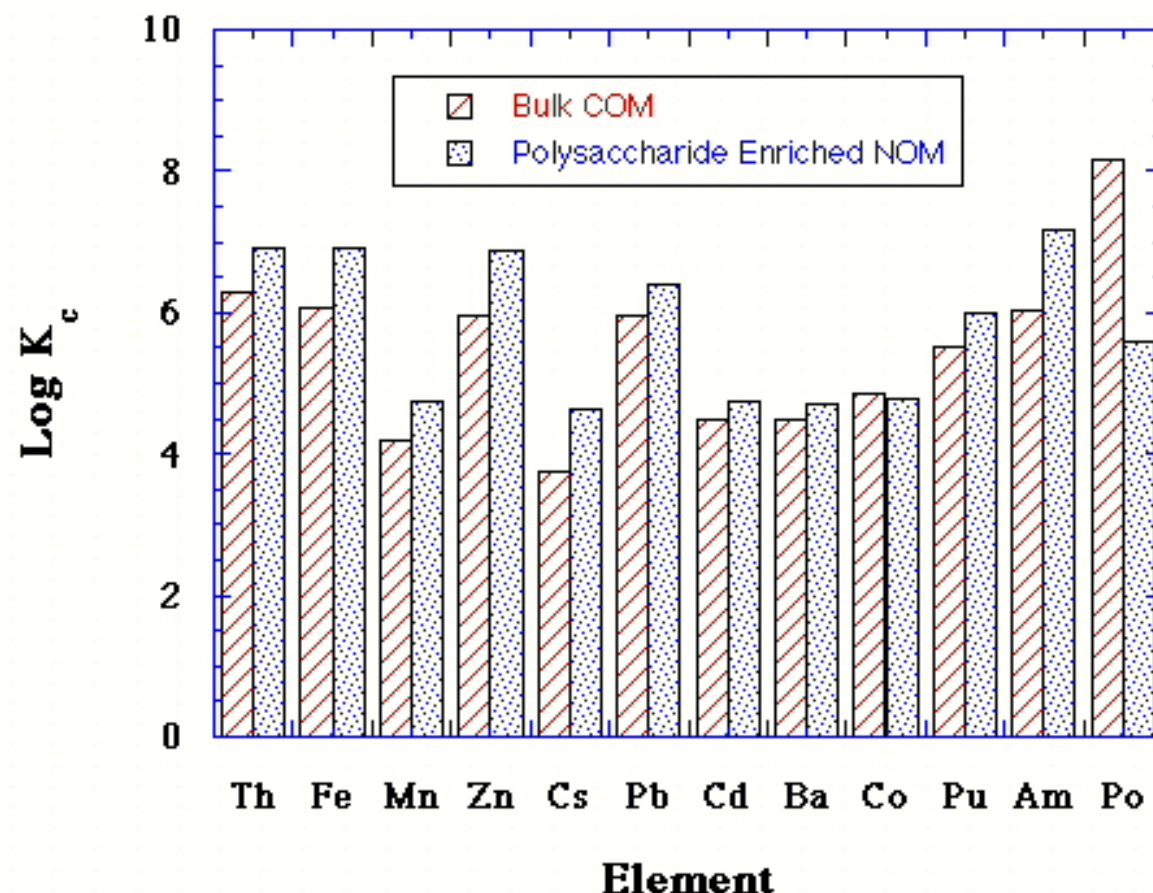


Abundance in ocean: CHO /POC ~ 0.1 , APS/POC ~ 0.01 , URA/POC ~ 0.01 (all: Santschi et al., 2003; Hung et al., 2003), Lig. /POC ~ 0.001 (Hirose, 2004); $^{234}\text{Th}/\text{Lig.} \sim 10^{-7} - 10^{-12}$

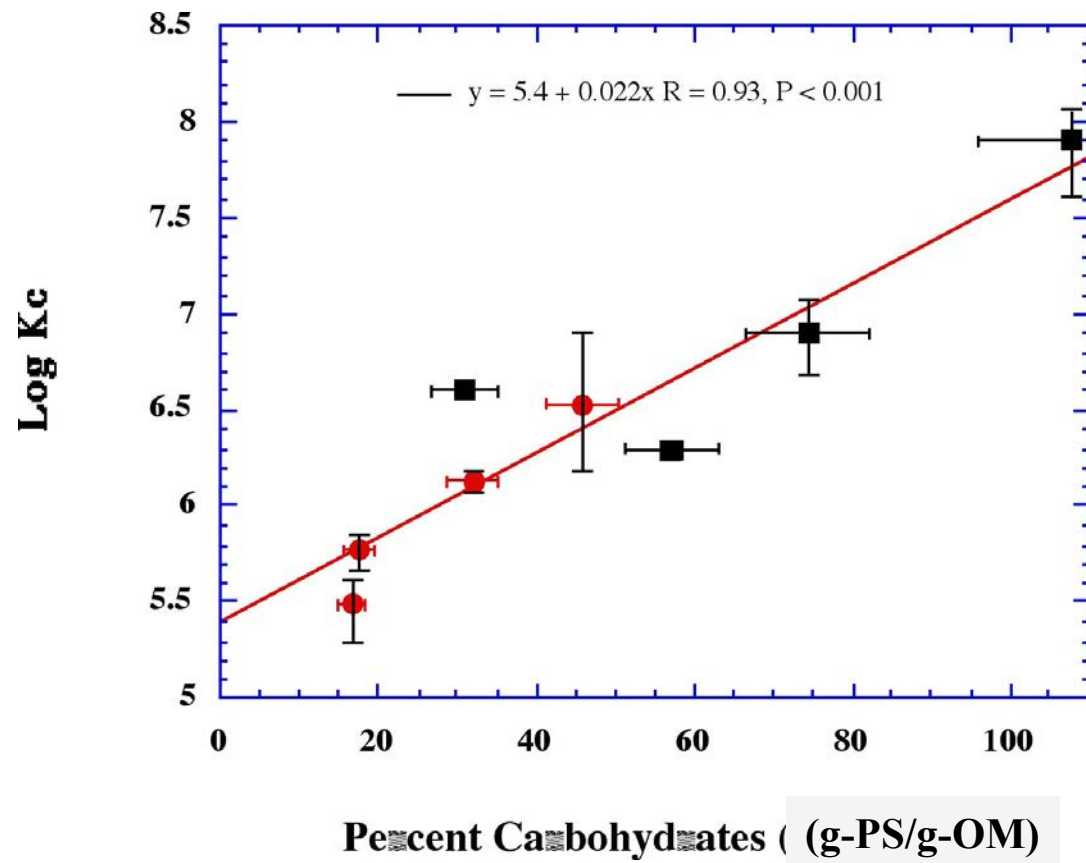


Different phytoplankton species appear, at times, to control acid polysaccharide (APS) e.g., uronic acid (URA), production and ^{234}Th (IV) complexation (-> autoporetic system)

Most Metals Show Enhanced Partitioning Coefficients (K_c) to Polysaccharide Enriched Colloidal Organic Matter (COM) over Unpurified COM (Quigley et al., 2002. L&O, 47, 367)



Colloid-Water Partition Coefficient (K_c) of $^{234}\text{Th}(\text{IV})$ controlled by Polysaccharide Content (Quigley et al., 2002. L&O, 47, 367)



$$K_c = K_c(0) \cdot 10^{(2.2f_{\text{PS}})}$$

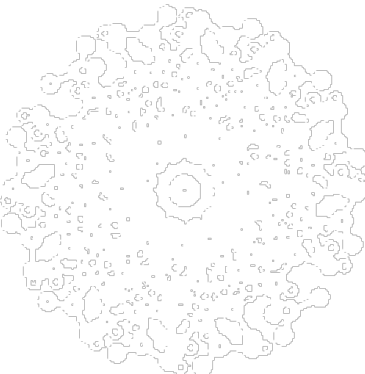
Enrichment
through
alcohol
precipitation



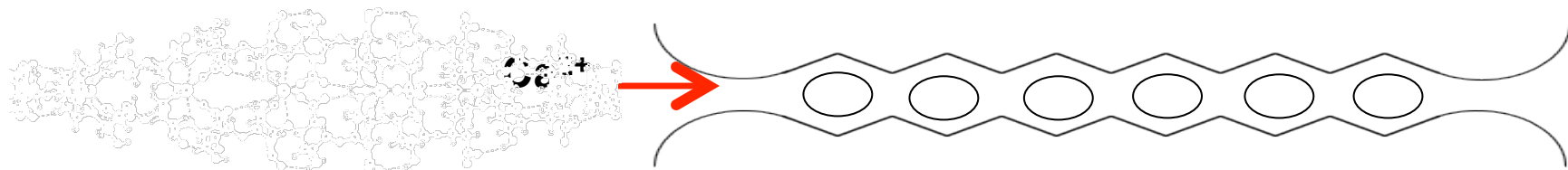
=>Increase in K_c and “freshness” ($\Delta^{14}\text{C}$)

Metal Binding (**chelation**) to Alginic Acid: Role of Ca^{2+} : Egg Box Model for Trace Metal Complexation in Acid Polysaccharides (-> “sheltering”)

Calcium poly- α -L-guluronate left-handed helix
view down axis

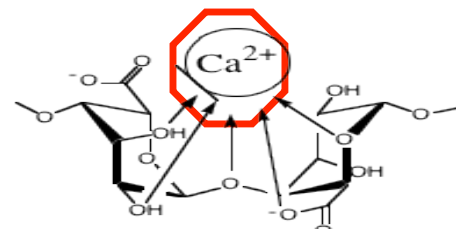


view along axis, showing the hydrogen bonding and calcium binding sites.



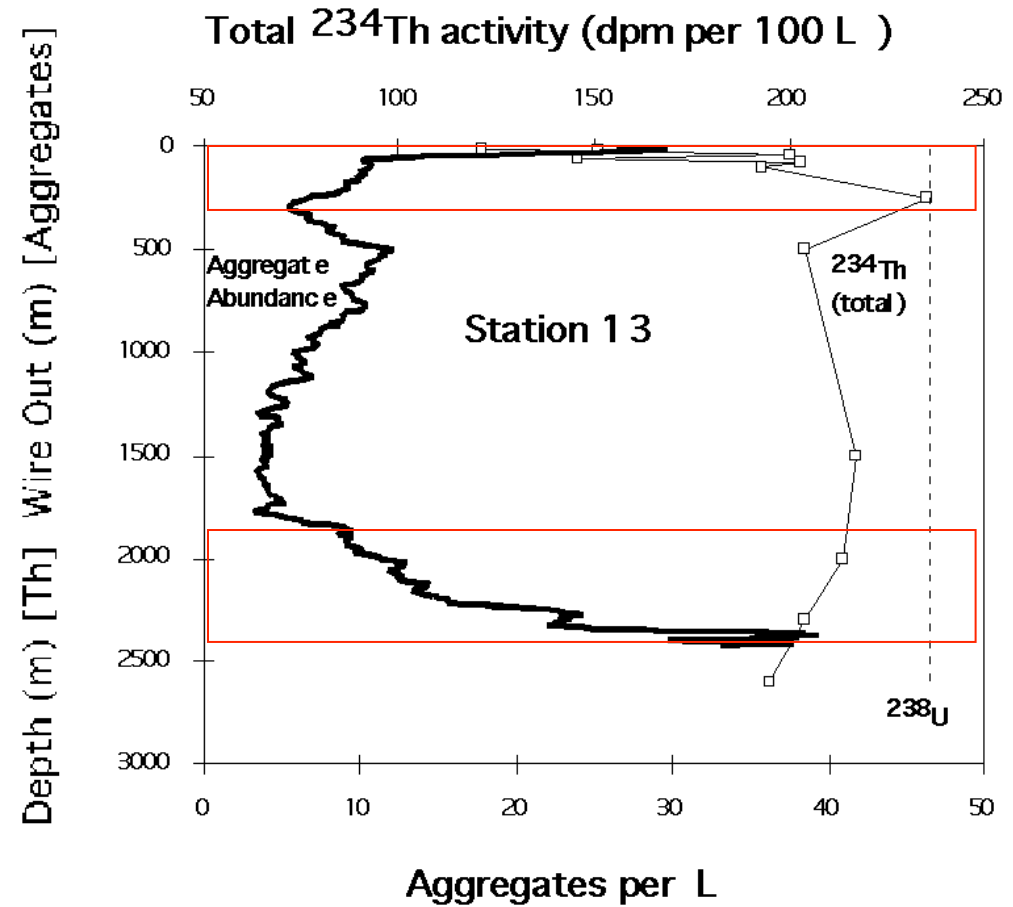
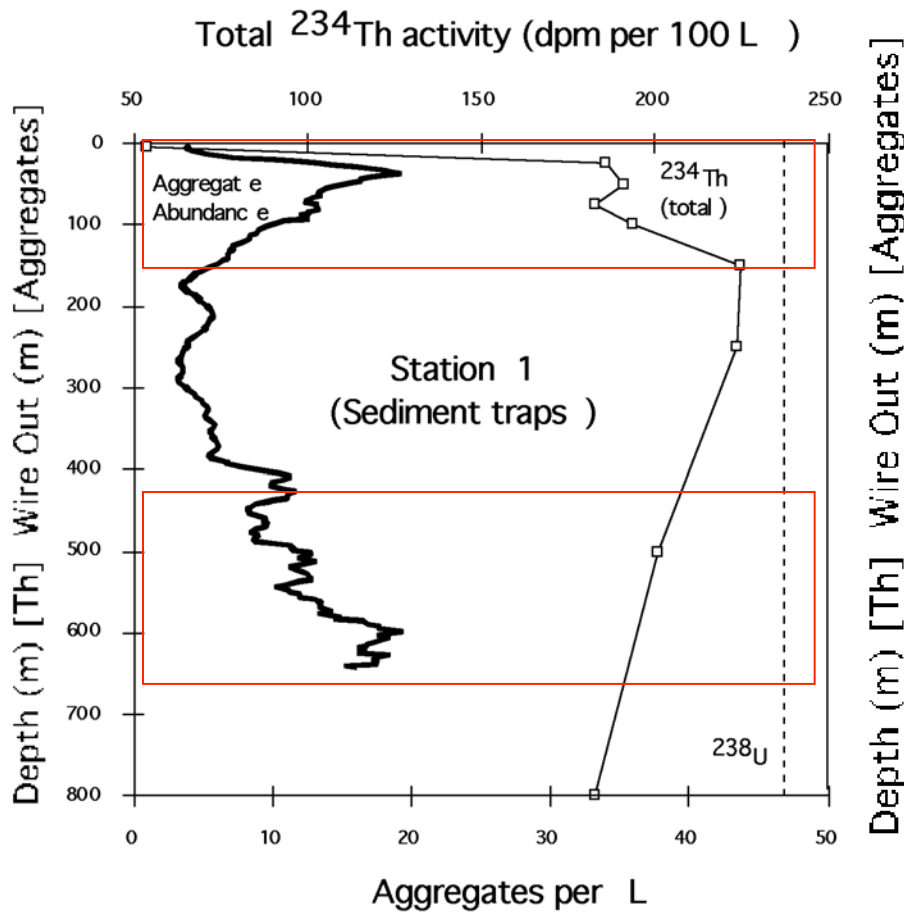
Alginic Acid

Double-helix **makes**
Molecule more rigid



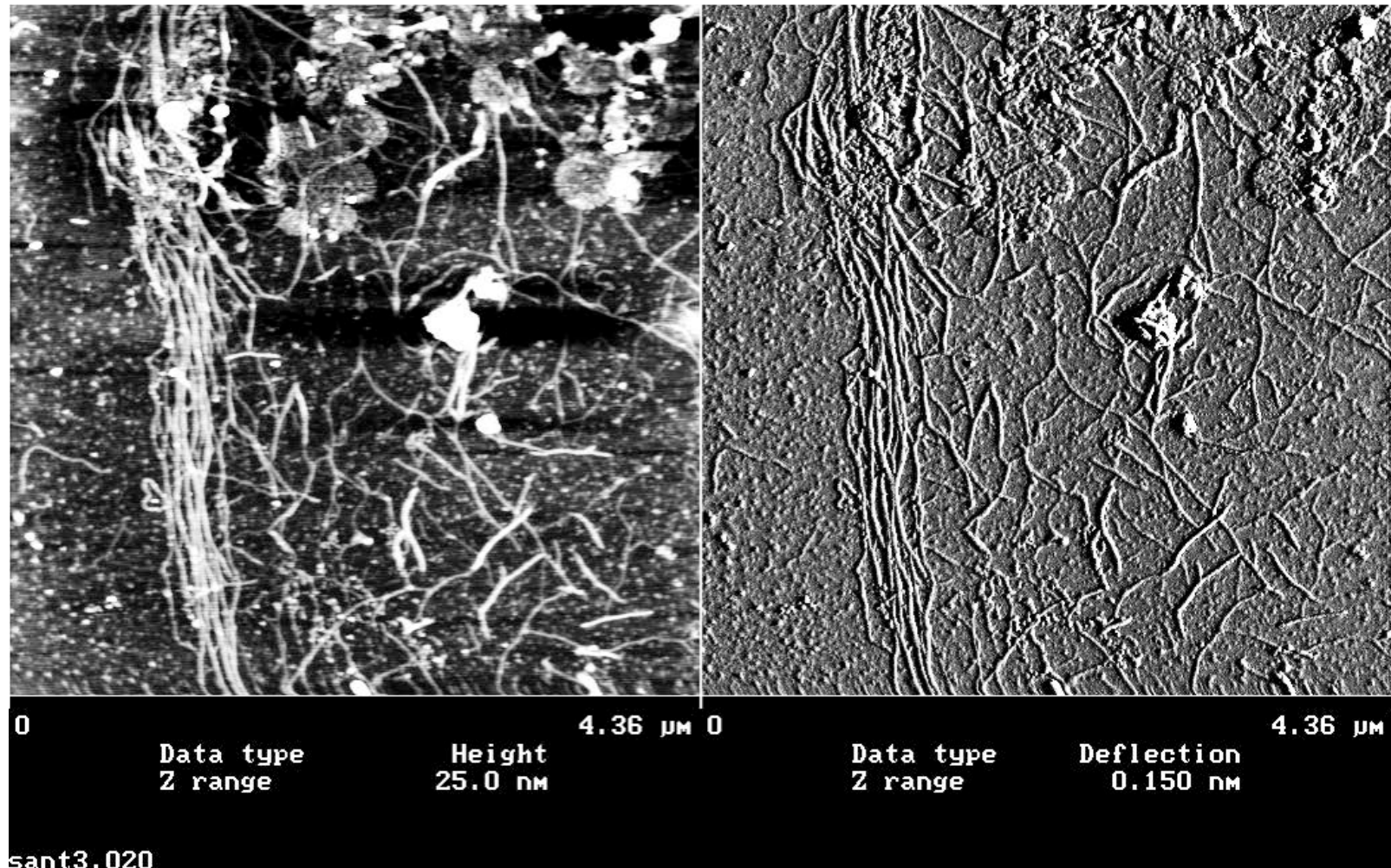
Ca^{2+} can be Replaced by other metals, e.g.,
 Fe(III) , Th(IV) , with similar ionic radii

^{234}Th deficiencies ($\sum(^{238}\text{U}-^{234}\text{Th})$) in the water column as a measure of particle scavenging intensity from vertical & lateral processes in surface and deep waters (Santschi et al., 1999, Cont. Shelf Res., 19, 609) Aggr~TEP~APS~EPS

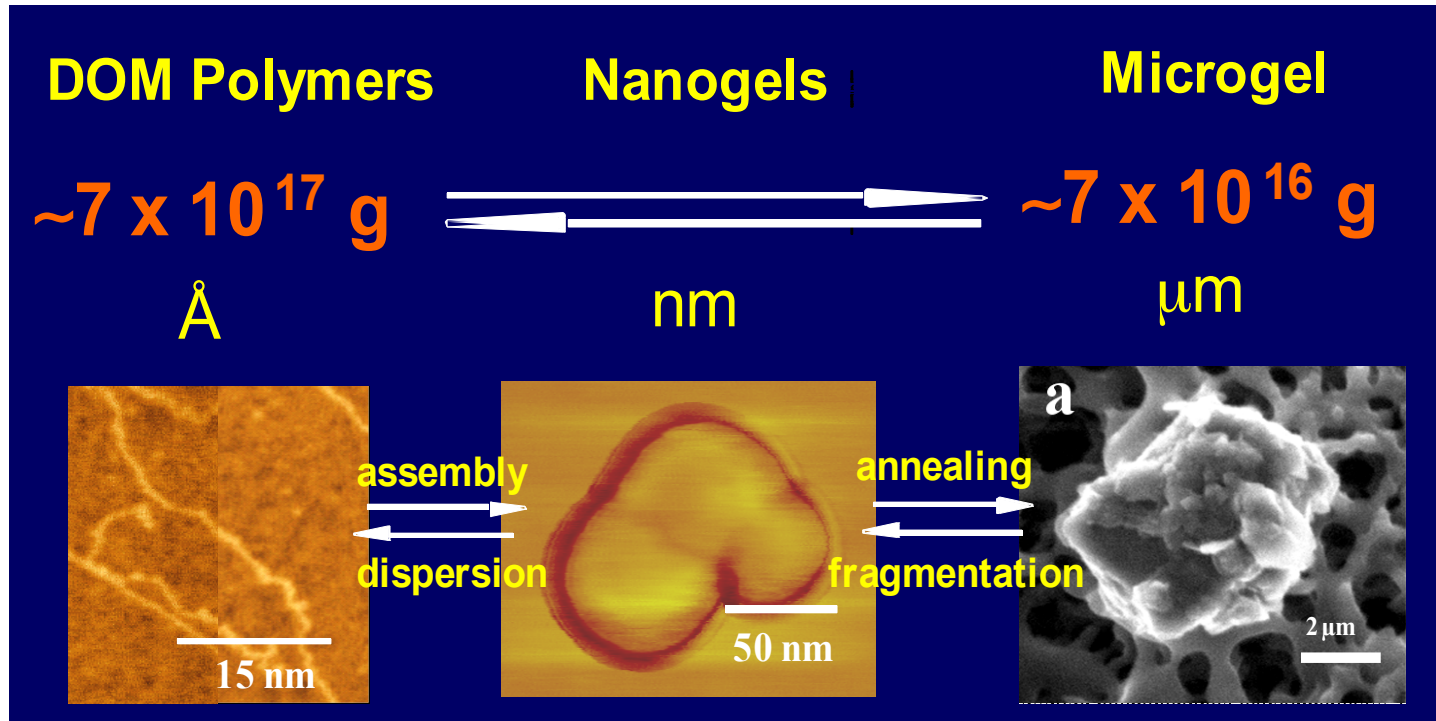


Abundance of Marine Snow Aggregates ≥ 1.5 mm dia α Th-deficiency

AFM image of fibrils from the Gulf of Mexico: Potential for
Gel Phase due to concentration/drying effects on the clay substrate (Santschi et al., 1998)



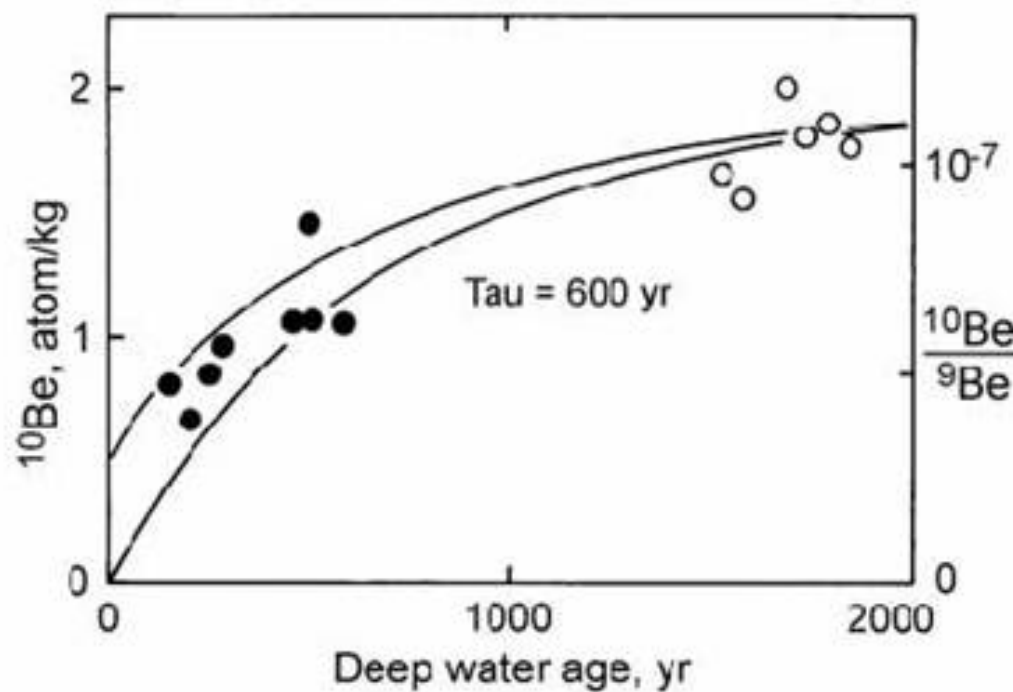
EPS from micro-organisms enhance gel-forming properties; hydrophilic EPS are held together by Ca²⁺-bridging (EDTA 'dissolves' them), EPS with hydrophobic moieties assemble through hydrophobic bridges; gel self-assembly as a two-step reversible process



Atomic force microscopy shows that during the first two hours following filtration, 0.2 μm -filtered seawater contain only free polymers that can be readily imaged on mica surface. After 5-10 hr nanogels start to appear. After 60 hr, assembly reaches equilibrium, forming microscopic gels of $\sim 4-5 \mu\text{m}$ that can be filtered and imaged by environmental scanning electron

Relationship between ^{7}Be and ^{234}Th in the ocean.

Oceanic residence time of Be is 10^3 yrs vs. that of Th which is 10^2 yrs



[89] Honeyman & Santschi: Brownian-pumping model 979

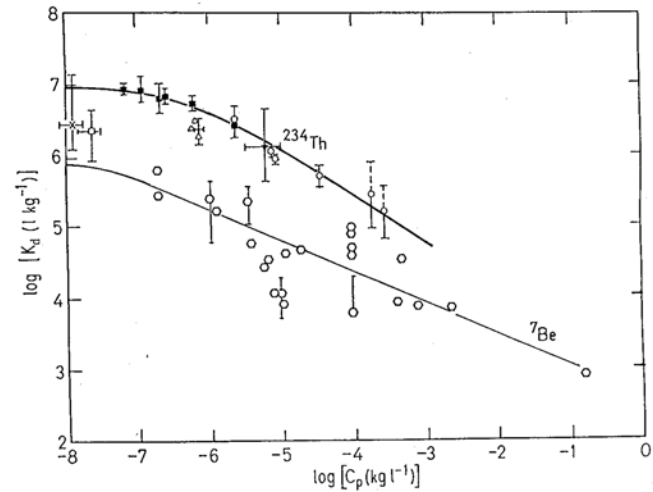


Figure 11. $\log K_d$ versus $\log C_p$ for $^{230,234}\text{Th}$ and ^{7}Be . Data: for Th: Coale and Bruland, 1985; McKee *et al.*, 1984; Santschi *et al.*, 1979; Minagawa and Tsunogai, 1980; after Honeyman *et al.*, 1988; for ^{7}Be : Li *et al.*, 1984; Nyffeler *et al.*, 1984; Hawley *et al.*, 1986; Buchholz, 1987; Bloom and Crecelius, 1983; Olson *et al.*, 1984; after Honeyman and Santschi, 1988. Relationships among master variables for model calculations correspond to those of Figure 9.

Left. Plot of ^{10}Be concentration against radiocarbon age in oceanic deep water to show the build-up of ^{10}Be along the Ocean Conveyer Belt. (!) = NADW; (") = Pacific deep water. After von Blankenburg *et al.* (1996). Right. Plot of particle-water partition coefficient vs. Particle Concentration (Honeyman and Santschi, 1989).

Complexation to Organic Templates?

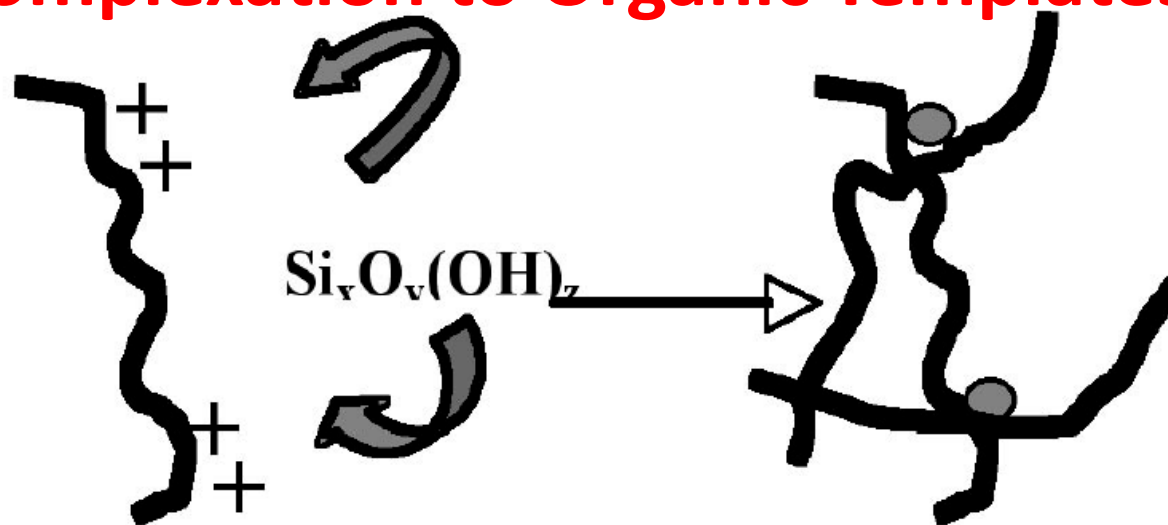


Figure 1: Self-assembling cationic biopolymers interact with anionic silicates to form silica nanoparticles.

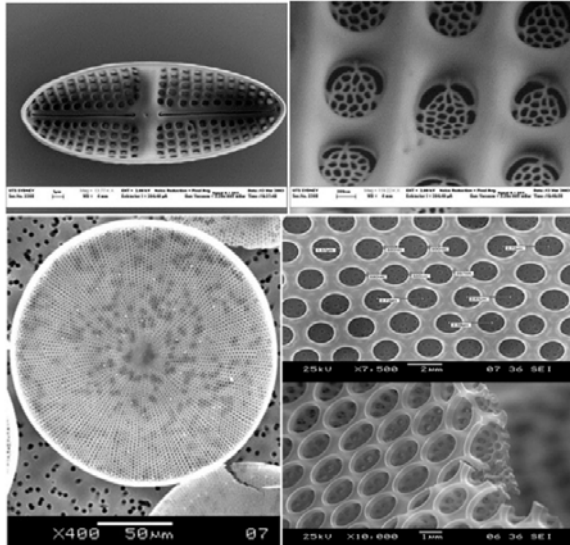


Fig. 4 Hierarchical distribution of pores in diatom frustules; Top: *Achnanthes subsessilis* (reprinted from Materials Science and Engineering C, 25, K.S.A. Butcher *et al.*, A luminescence study of porous diatoms, 659, Copyright (2010), with permission from Elsevier); Bottom: *Coscinodiscus walesii* (reprinted from ref. 77, Copyright (2010), with permission from Elsevier).

Silaffins as templates for nano-silica growth of diatom shells -> organic residues as binding agents of natural radionuclides to diatoms (rather than pure silica which is a poor sorbent)

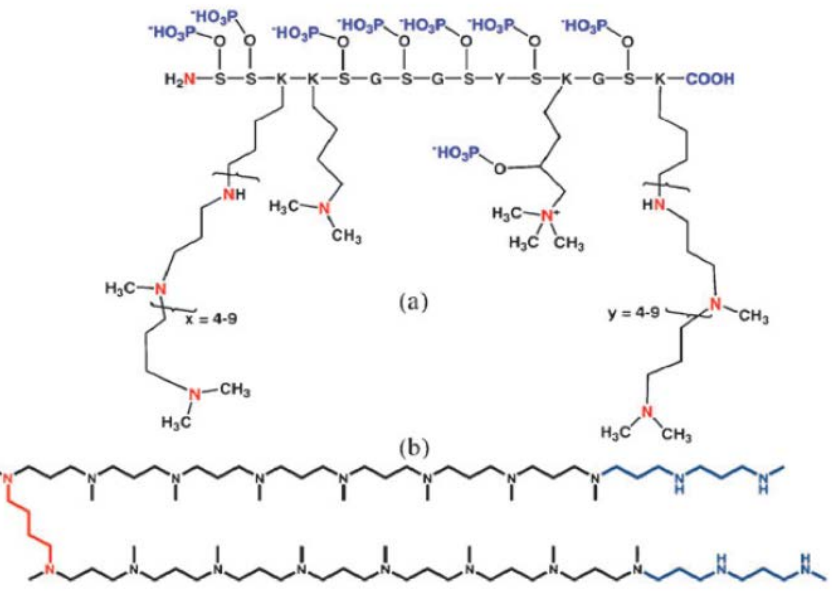


Fig. 5 Molecular structure of (a) silaffins and (b) LPA.

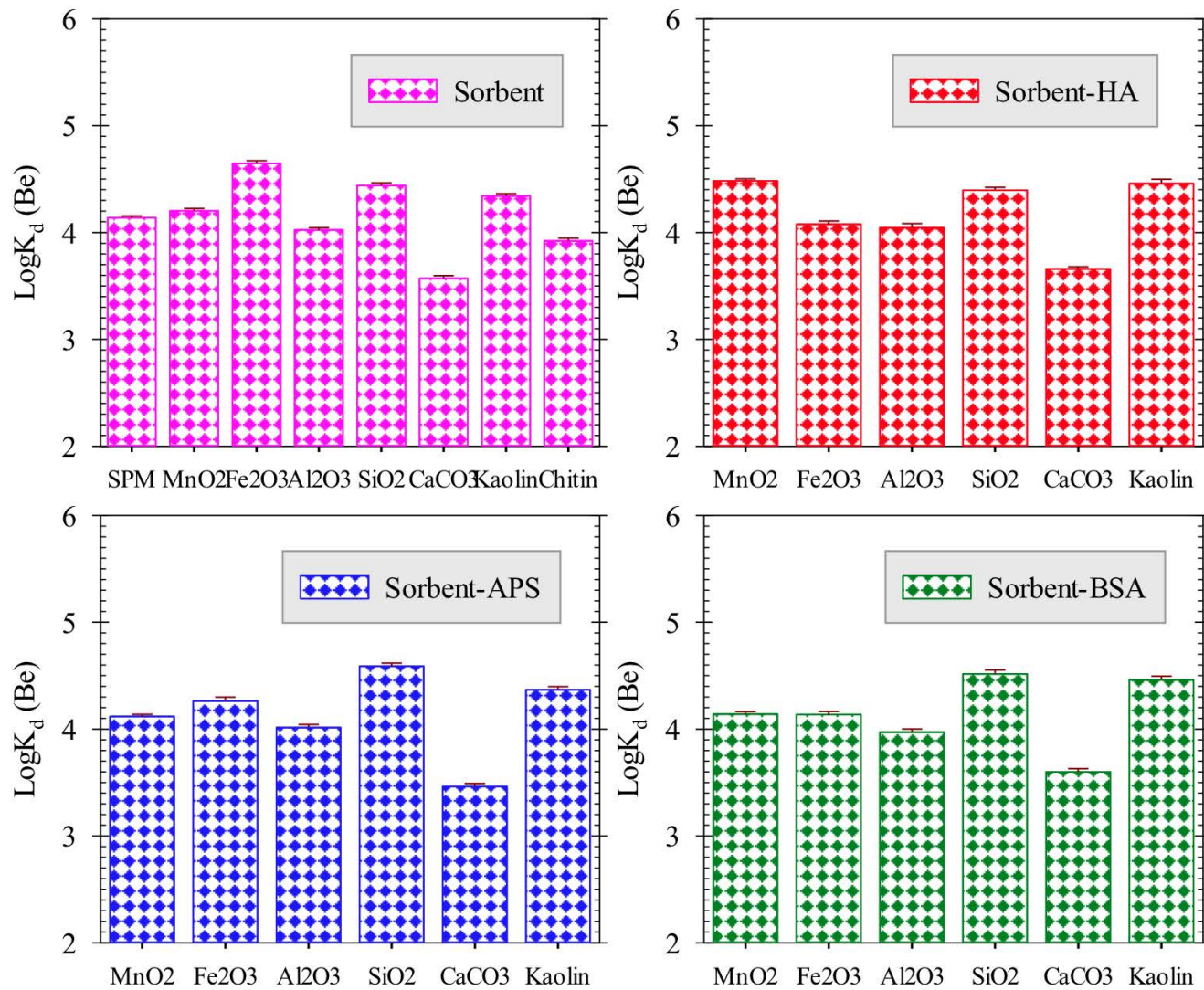
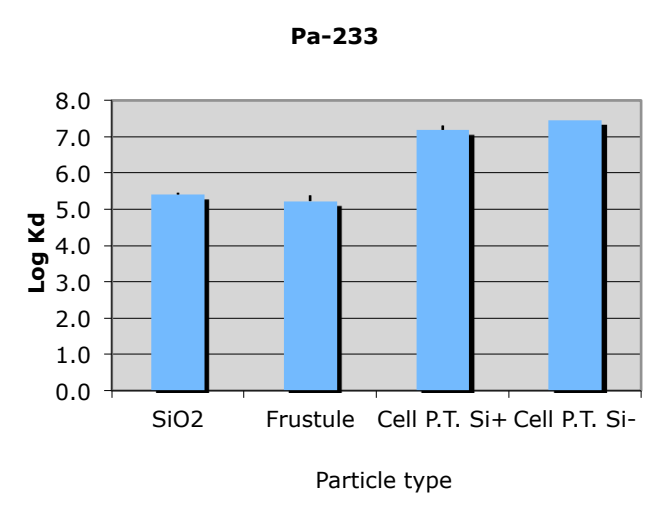
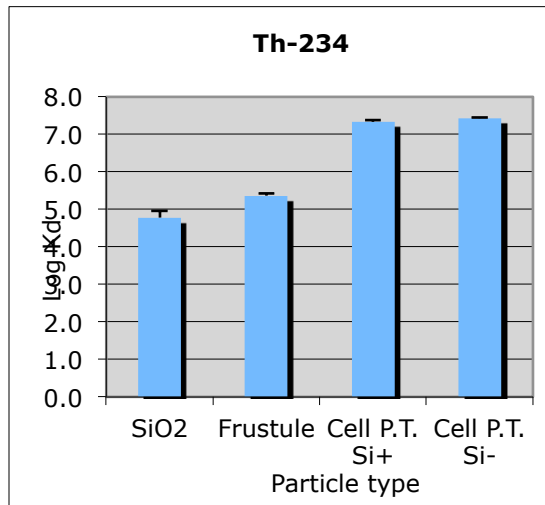
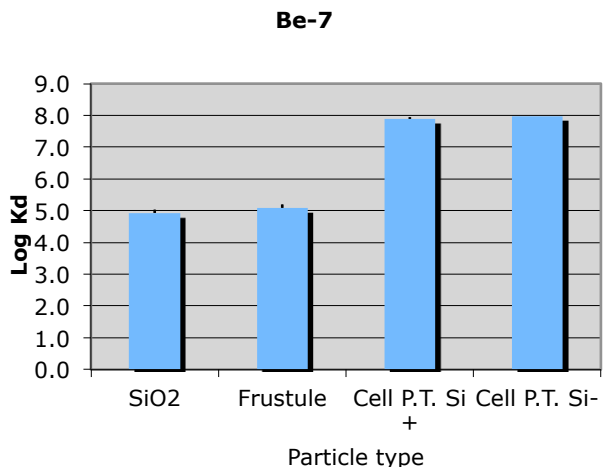


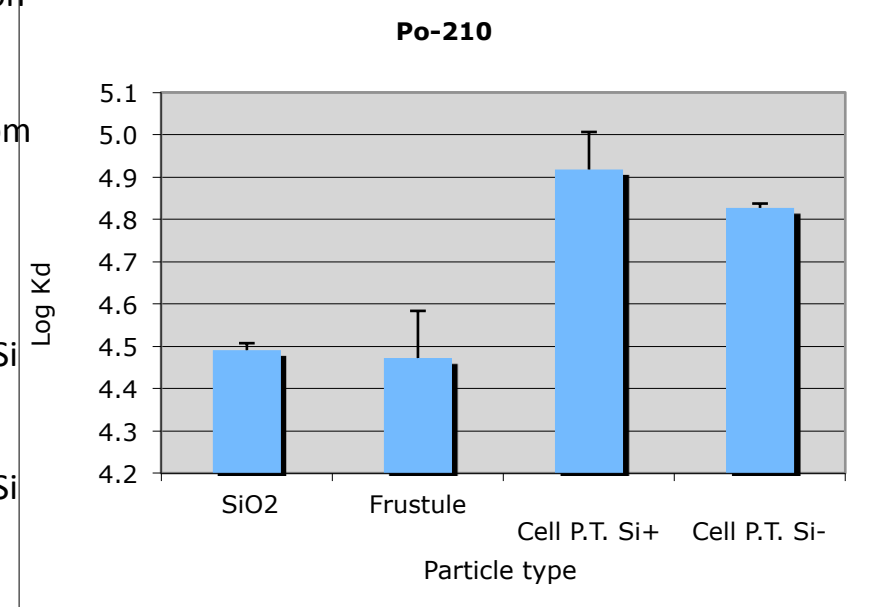
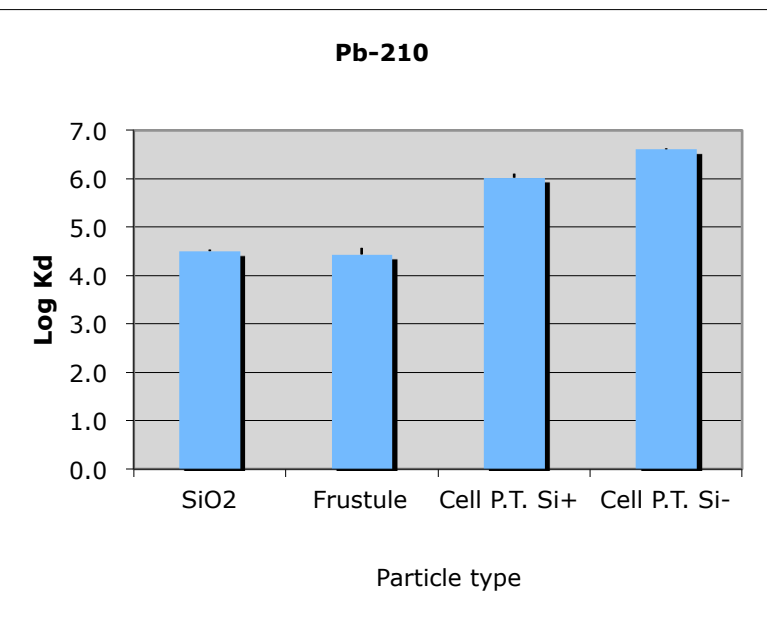
Fig. 3 Partitioning coefficients (K_d) of ^{7}Be on different particle types

Weifeng Yang, Laodong Guo, Peter H. Santschi, unpublished results



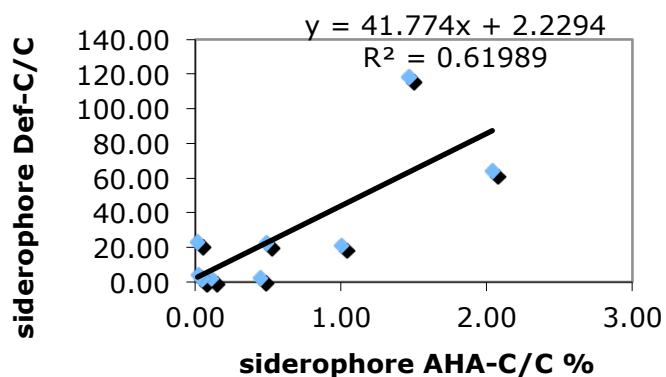
- Kd sequence **Be>Th>Pa>Pb>Po**
- SiO₂~cleaned Frustule<Cells P.T.

Treatments
inorganic particle
SiO₂
Diatom,
Phaeodactylum tricornutum
Frustules (Carbon content < 1%)
B) Fresh
uncleaned diatom cells (P.T. = *Phaeodactylum tricornutum*)
1. diatom cultured under Si+ (with Si shell)
2. diatom cultured under Si- (without Si shell)

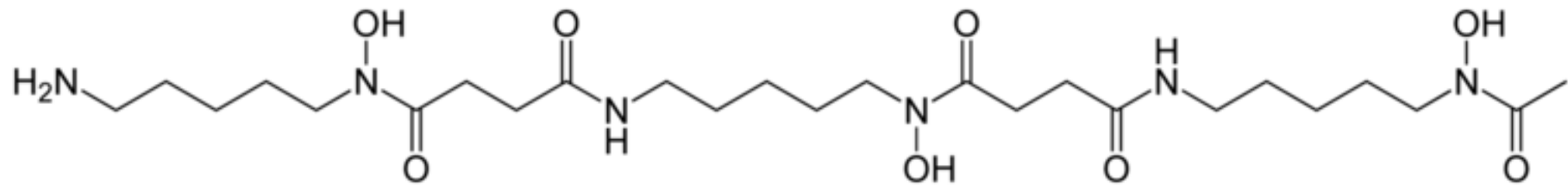


**Anderin Chia-Ying Chuang,
unpublished results**

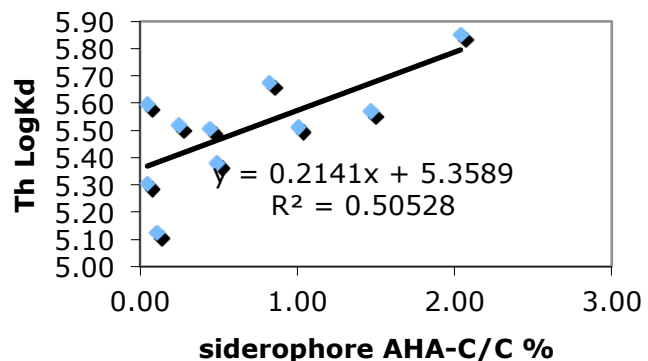
EPS&Colloids



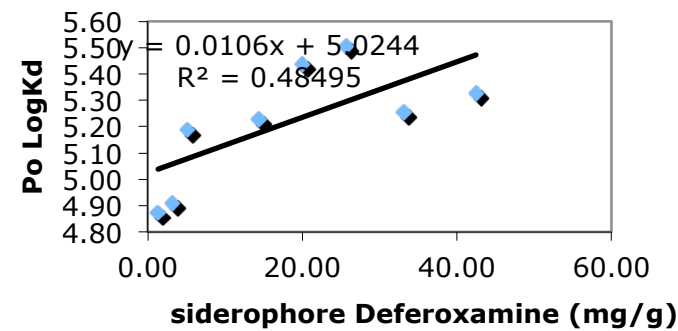
No relationships for Be, Pa and Pb; Anderin Chia-Ying Chuang, unpublished results



Colloids

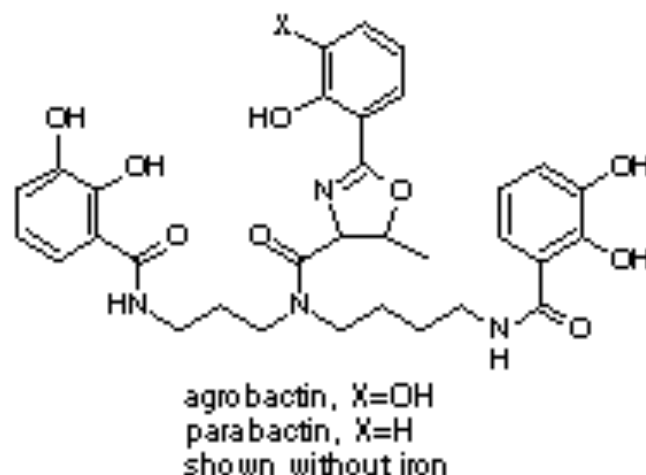
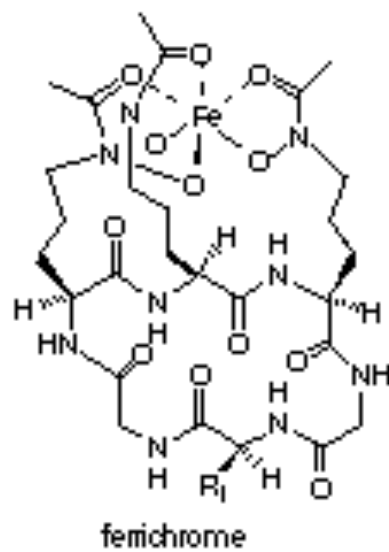
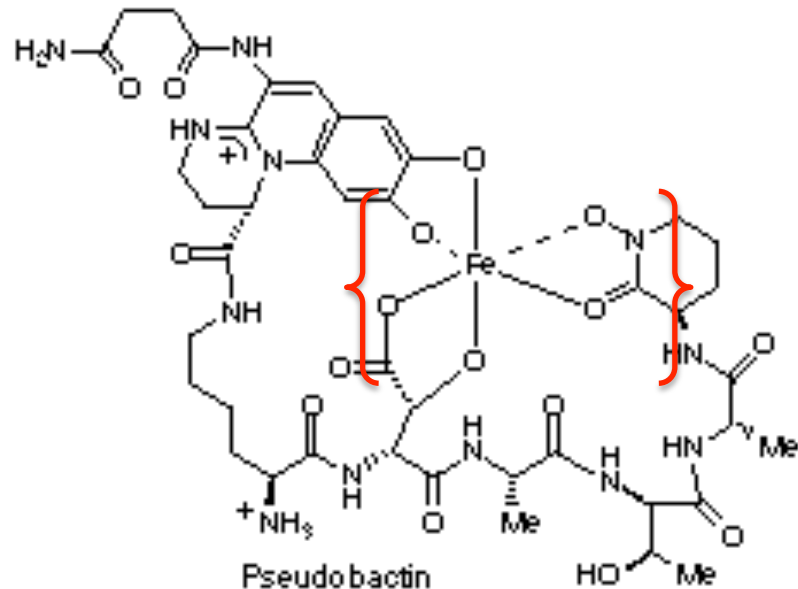
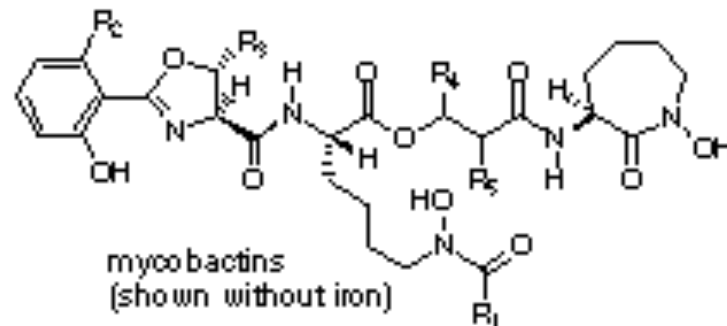


Colloids



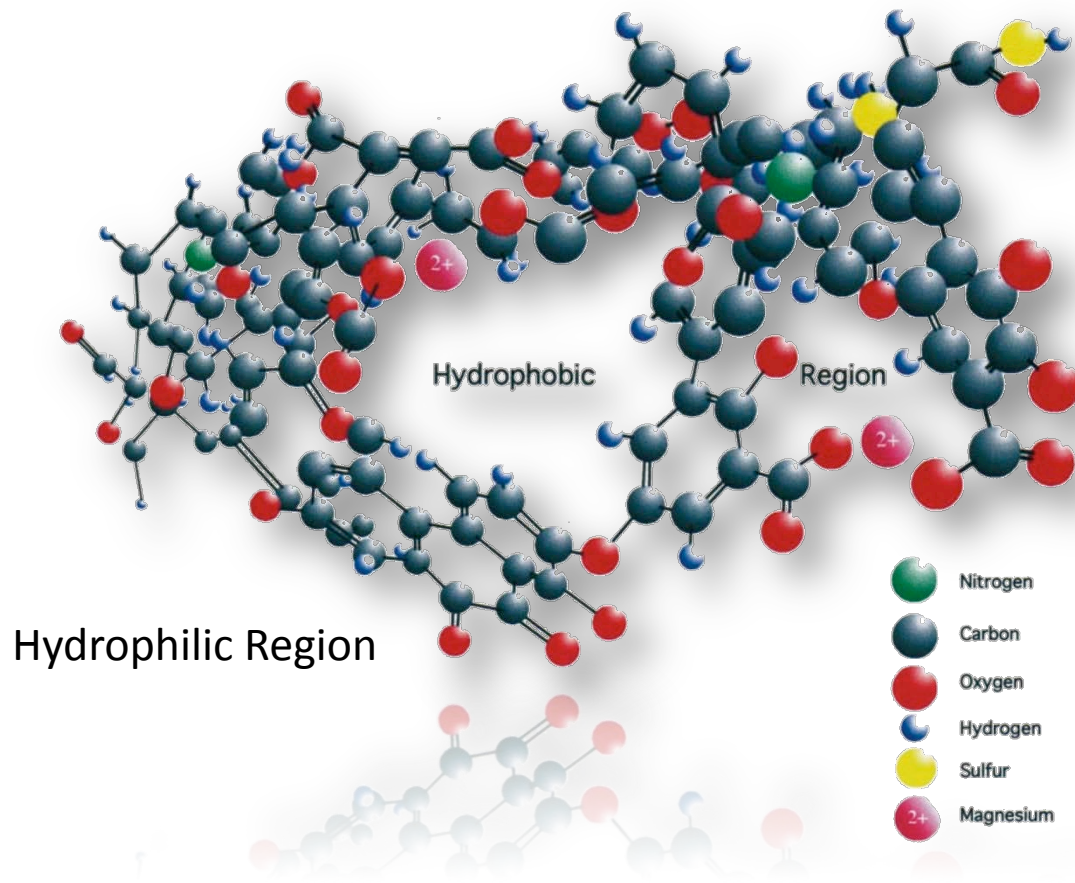
Siderophores

Representative Siderophores:



“All-In-One” Bio-polymers or Geopolymers as carriers of natural (Th, Pa, Pb, Po, Be) radionuclides in aquatic systems

Example: Humic Acid molecule



- Have hydrophilic outside, hydrophobic interior
- Contain metal binding (chelating) groups
- can act as electron shuttles (e.g., quinone-hydroquinone or flavone groups)

Example: Humic Substance

supramolecular association of self-assembling heterogeneous and relatively small molecules derived from the degradation and decomposition of dead biological materials, stabilized predominantly by weak dispersive forces, such as hydrophobic and hydrogen or Ca^{2+} binding.

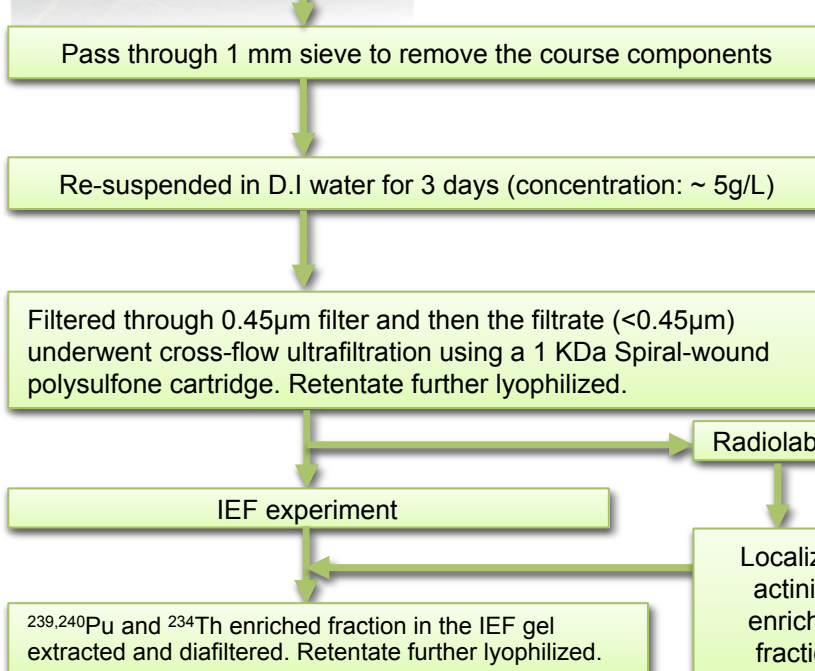
Separation methods and schemes

- Isoelectric focusing, Ultrafiltration, HPLC, ion chromatography, alone or in combination.

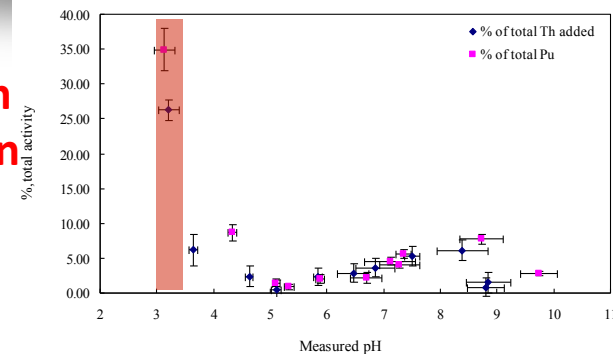
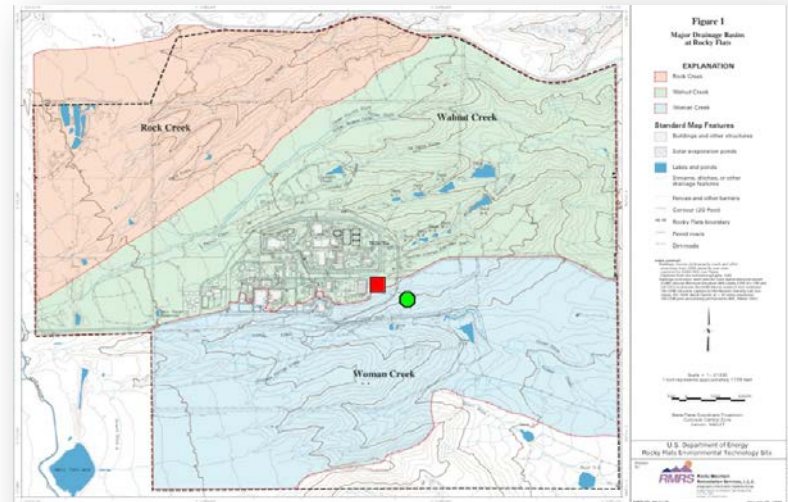
Chemical Characterization Methods:

- GC-MS, HPLC, ATR-FTIR, NMR, ...

**Examples for $^{239,240}\text{Pu}$ (and ^{129}I)
from contaminated sites:
Characterization after IEF, UF,
and/or HPLC separation**



Plutonium Separation Via IEF



Graphite AA
(Fe, Mn, Al)

Elemental mapping

ATR-FTIR

Compositional analysis (TCHO, URA, protein, etc.)

HPLC-SEC

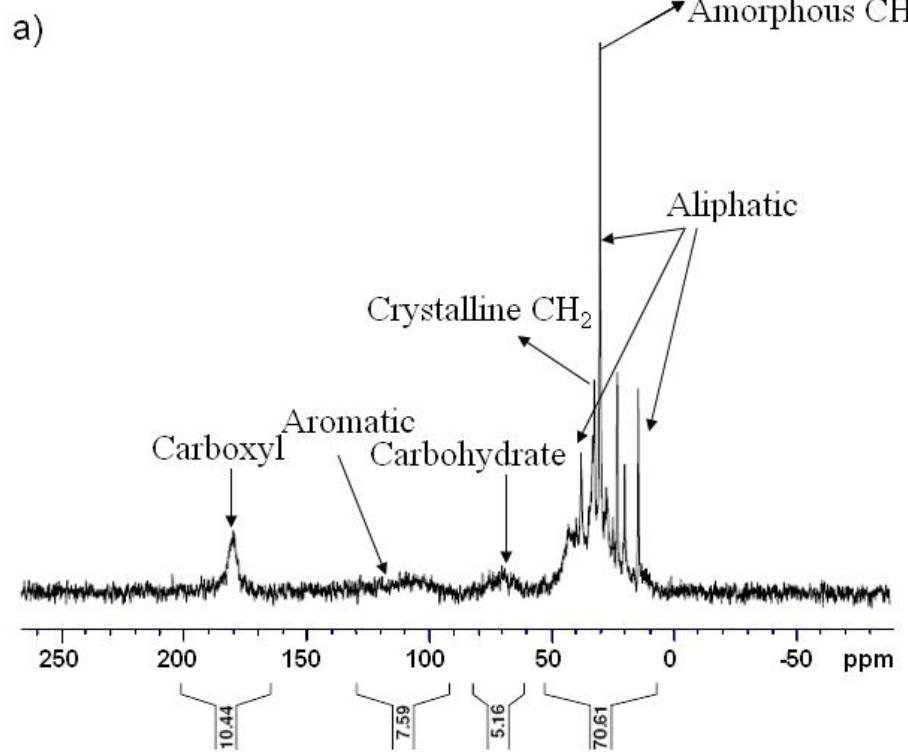
Elemental analysis

NMR

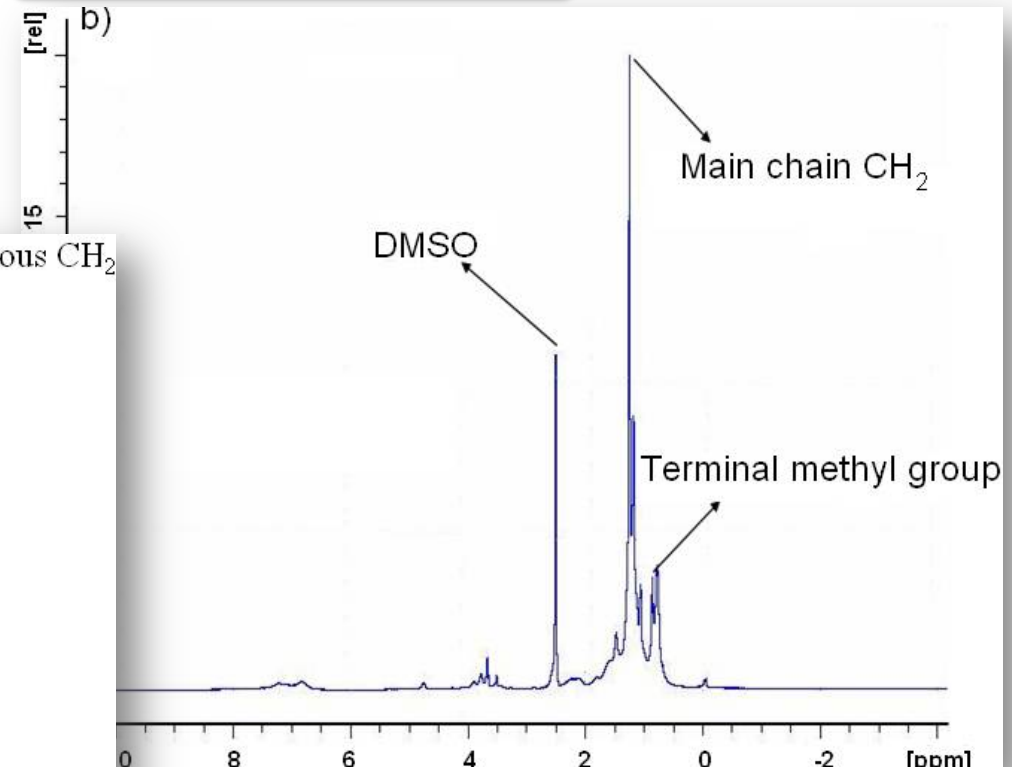
1D ^{13}C and ^1H NMR



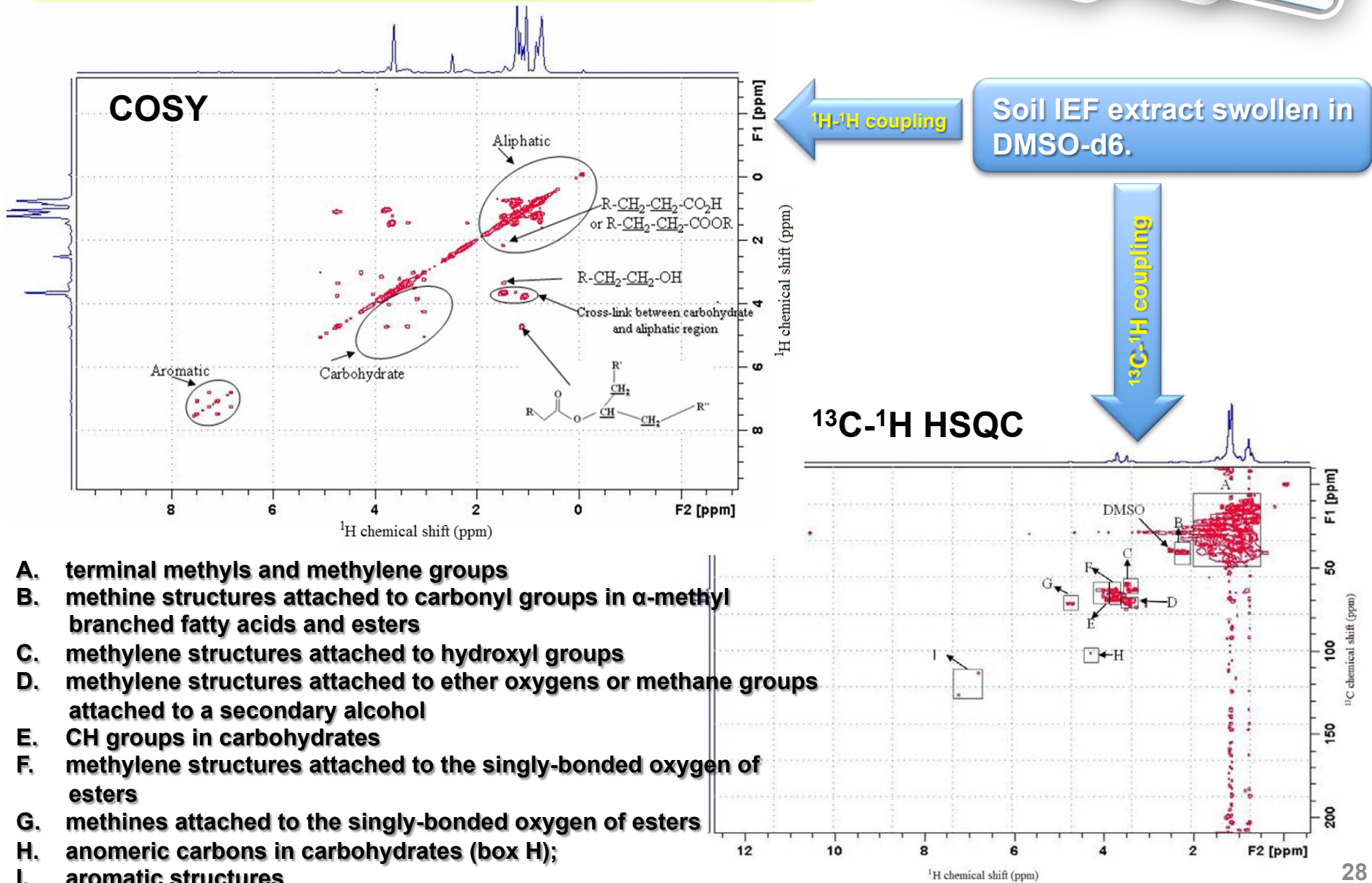
DPMAS ^{13}C NMR



^1H HRMAS-NMR



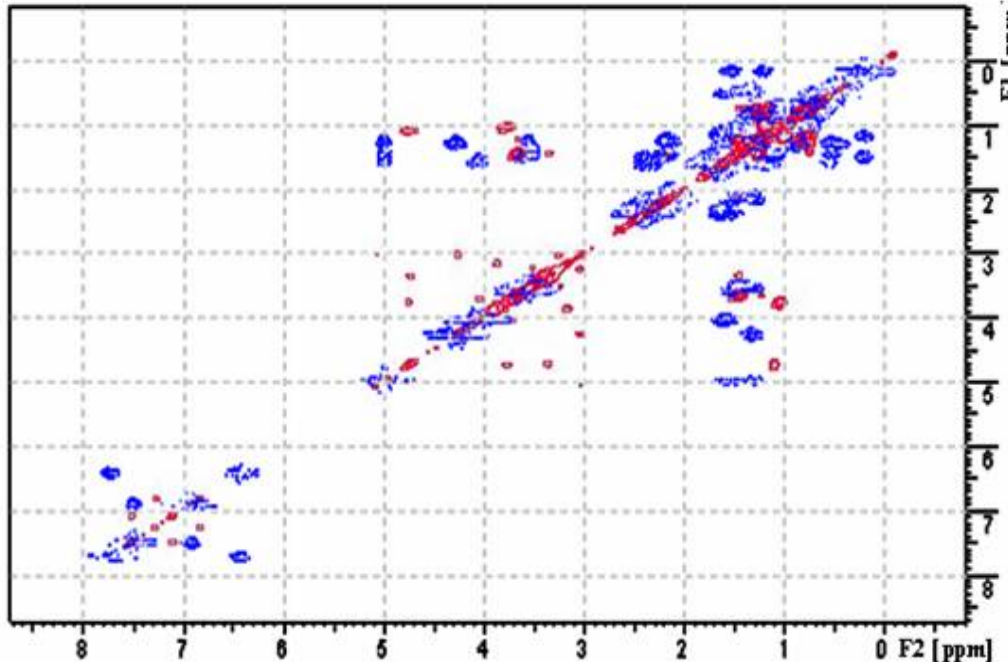
2D NMR



Simulation and overlapping

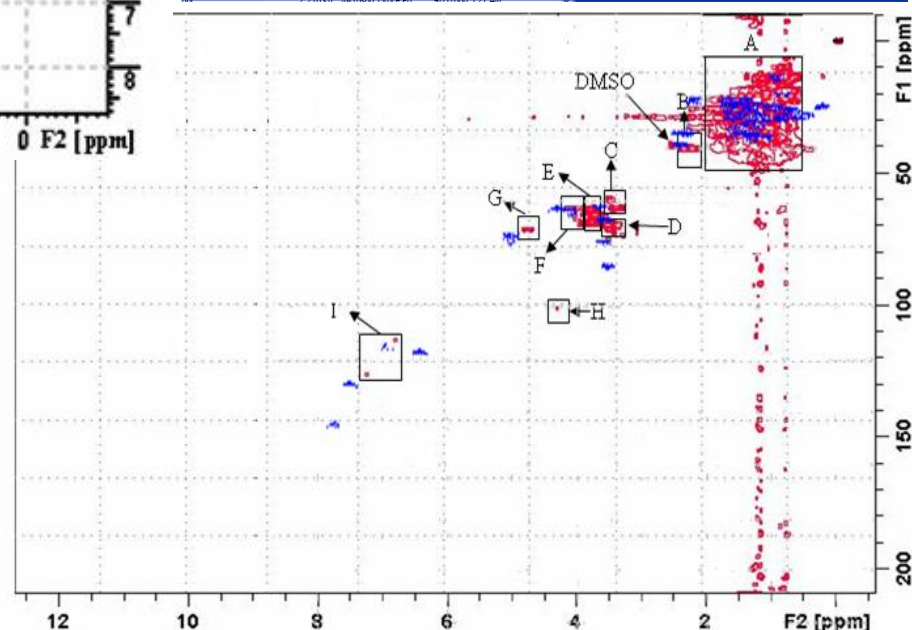
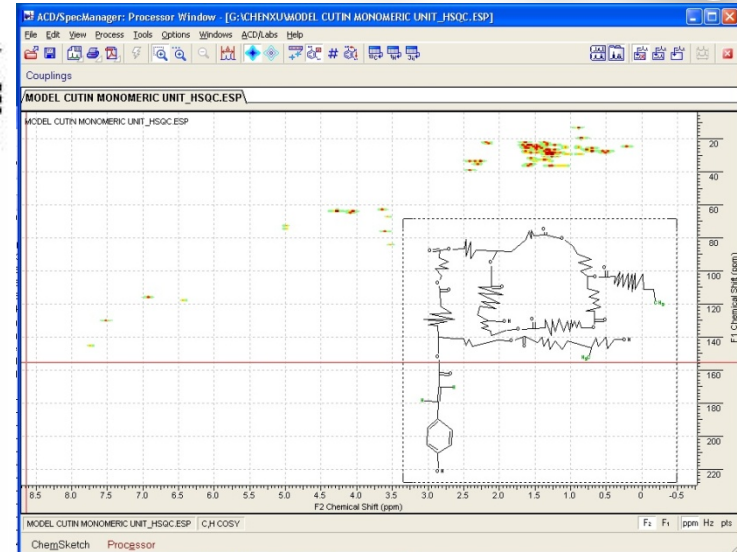


d)



Overlapping with

- published cutin NMR spectra (Kelleher and Simpson, 2006, ES&T; Deshmukh, Simpson and Hatcher, 2003, Phytochem)
- simulated NMR spectra of proposed cutin models (Fang et al., 2001, Phytochem; Kolattukudy, 2001)



Siderophore attached to cutin backbone

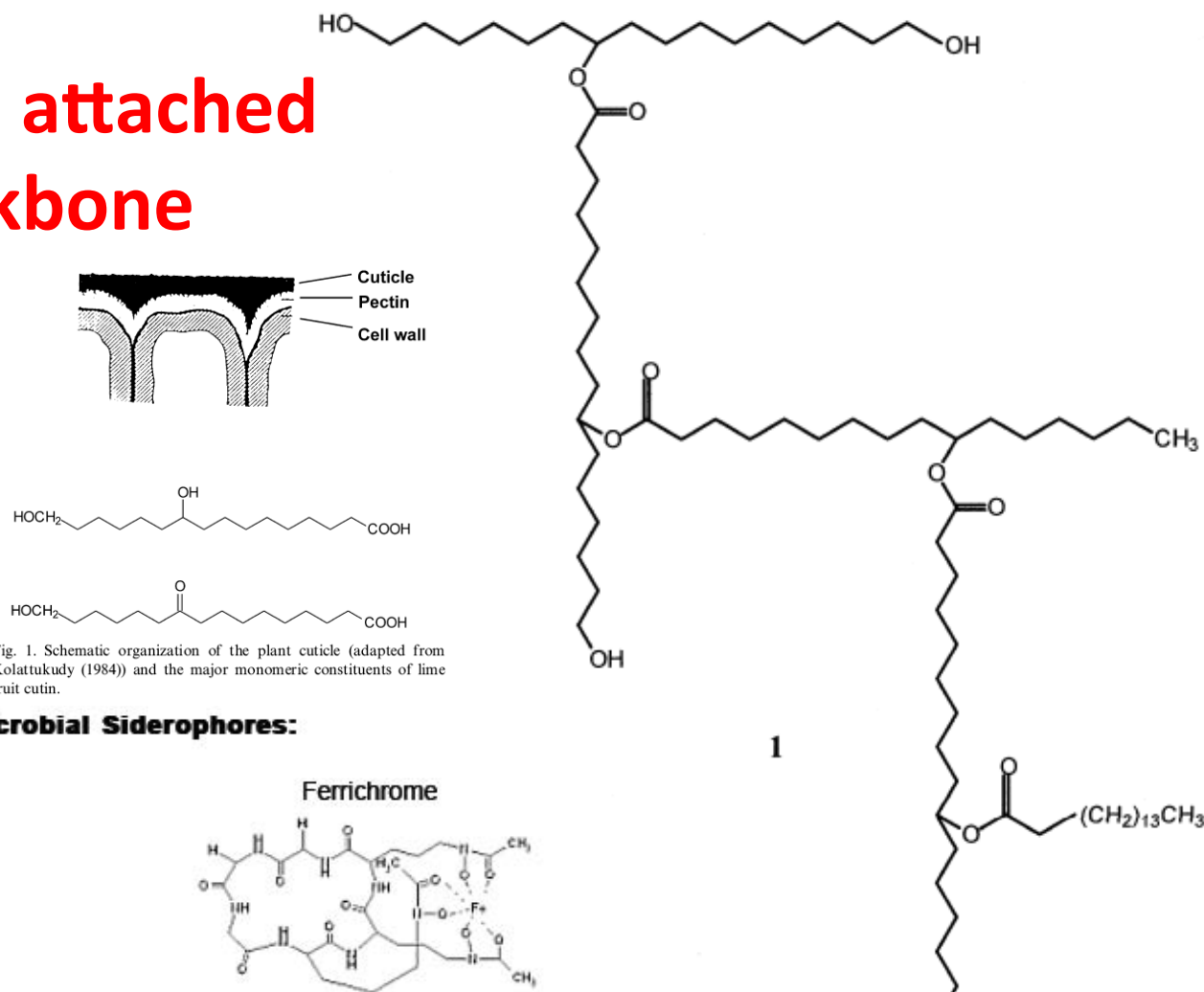
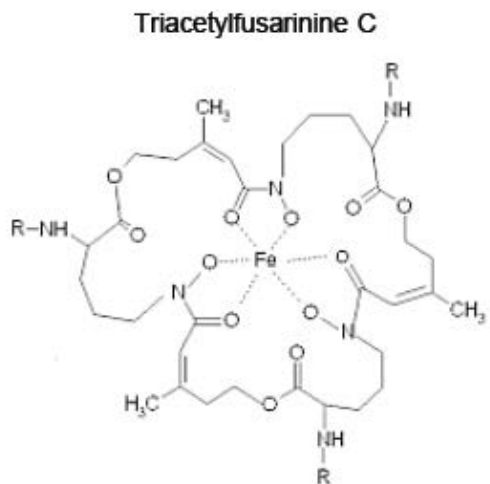
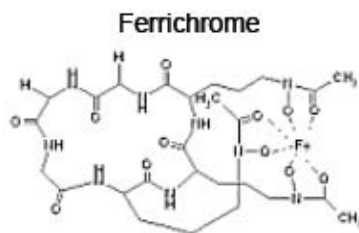


Fig. 1. Schematic organization of the plant cuticle (adapted from Kolattukudy (1984)) and the major monomeric constituents of lime fruit cutin.

Common Microbial Siderophores:



Coprogen



Ferrioxamines

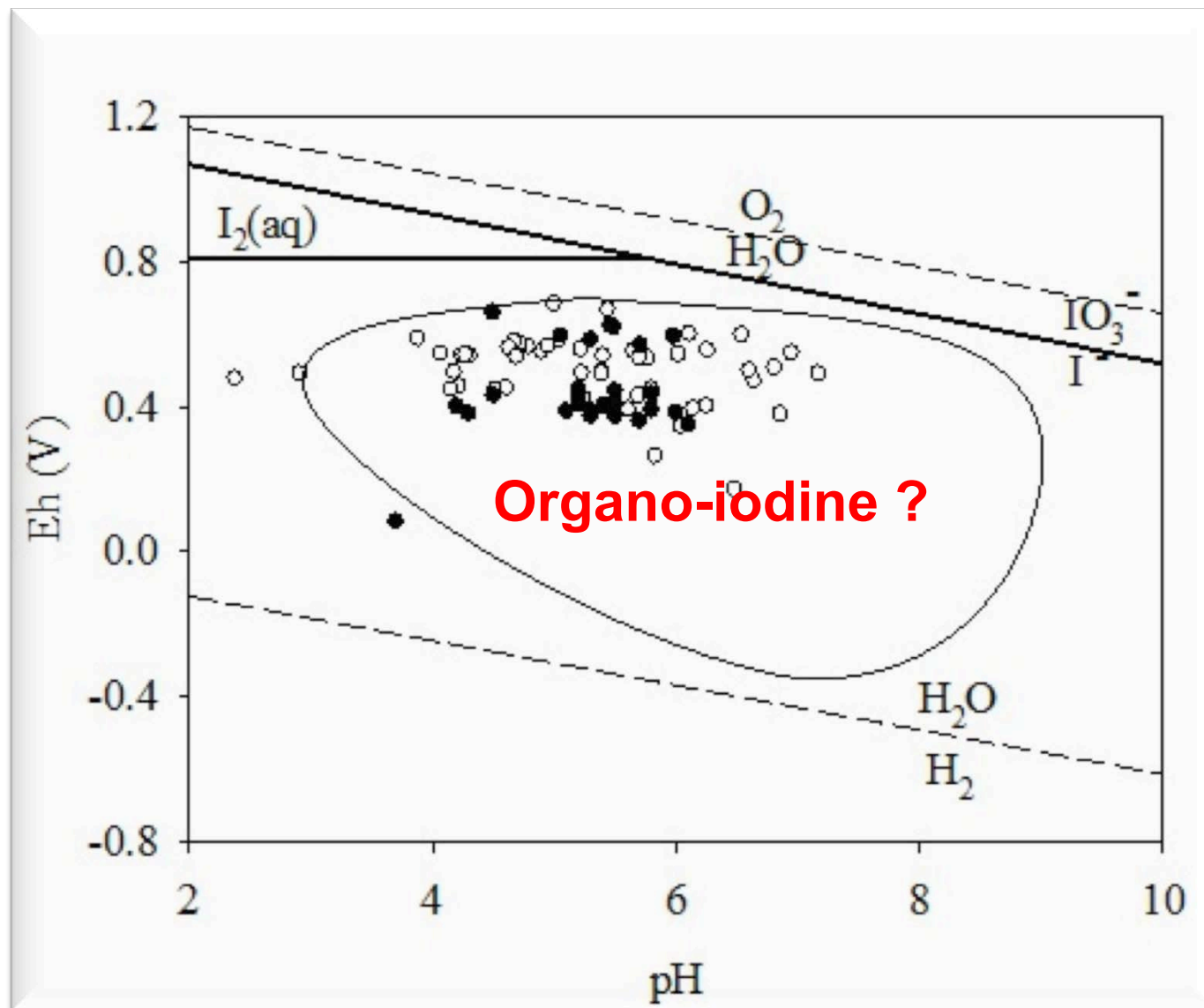
Conclusions

- Radionuclides in the environment can often find **chelating** and **redox active** bio- or geo-polymers because their ultra-low concentrations allow them to find the most energetic sites. For example, ⁷Be can show high Kd values to diatoms containing silafins.
- Separation chemistry combined with organic chemical methods allow **identification of carrier molecule(s)** for radionuclides (e.g., P, Th, Po) containing strongly chelating groups (hydroxamates, siderophores), anionic coatings (polysaccharides), and hydrophobic backbones (cutins).
- Organic carriers of radionuclides in the environment are likely also affecting or could be responsible for observed fate, effects, and interpretation of historical reconstructions.

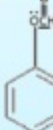
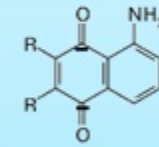


**Thank you for your attention
Any questions ?**

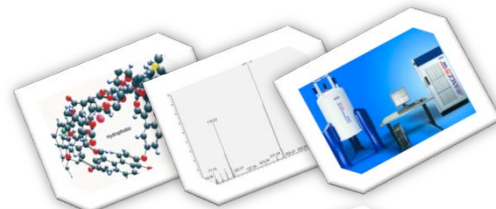
pH-Eh of Iodine.



Evidence for Iodine bound to aromatic carbon from NMR and I- (or IO3-) binding (Kd) experiments (Xu et al., 2011a,b)

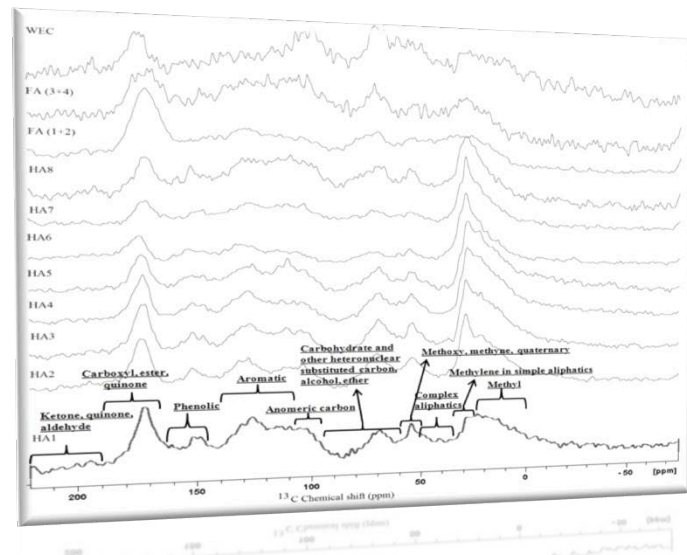
Proposed active aromatic ring for iodine binding*	^{13}C (ppm)	^1H (ppm)
	173.0	7.06-7.41
	171.39	7.08-7.58
	185.2-188.2	7.17-7.65
	160.2	7.92-7.94, 8.29

Structural relevances to naturally occurring and laboratory-iodination

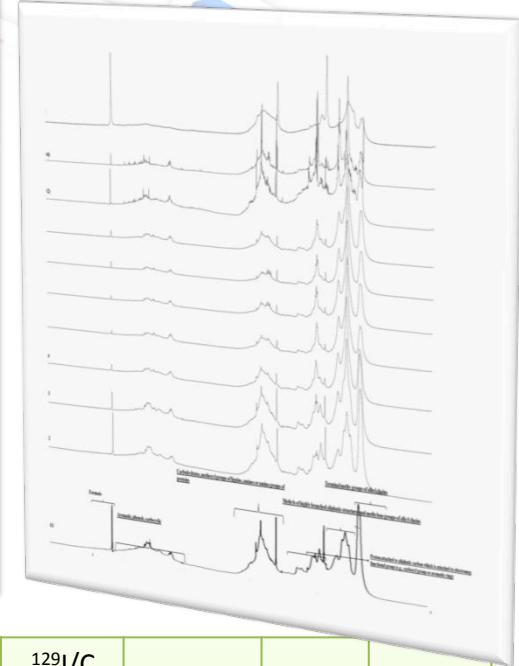


Functional group	Chemical shift (ppm)	$^{127}\text{I}/\text{C}$ $\mu\text{g/g-C}$		$^{129}\text{I}/\text{C}$ $\mu\text{g/g-C}$		Kd (g/ml)	
		R ²	p	R ²	p	R ²	p
C _{Alk-H,C}	0-60	-0.610	-*	-0.607	-	-0.871	-
C _{Alk-O}	60-108	0.055	-	0.053	-	0.003	-
$\Sigma \text{C}_{\text{Alk}}$	0-96	-0.289	-	-0.339	-	-0.715	-
C _{Ano}	96-108	-0.189	-	-0.020	-	-0.004	-
C _{Ar-H,C}	108-145	0.226	-	0.420	-	0.523	0.028
C _{Ar-O}	145-162	-0.186	-	-0.209	-	-0.066	-
$\Sigma \text{C}_{\text{Ar}}$	108-162	0.100	-	0.243	-	0.449	0.048
C _{COO}	162-190	0.774	0.030	0.711	-	0.882	<0.001
C _{C=O}	190-220	-0.043	-	-0.196	-	-0.056	-
C _{Ar-H,C} x C _{COO}	(108-145)×(162-190)	0.576	0.017	0.665	0.007	0.890	<0.001

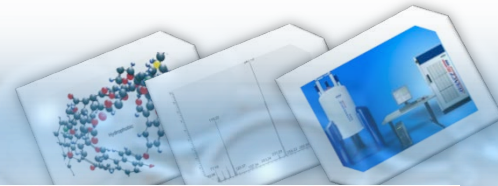
*"-p values were not reported



Functional group	Chemical shift ppm	$^{127}\text{I}/\text{C}$ $\mu\text{g/g-C}$		$^{129}\text{I}/\text{C}$ $\mu\text{g/g-C}$		Kd	
		R ²	p	R ²	p	R ²	p
H _{CH₃}	0-1.67	-0.853	-	-0.714	-	0.660	-
H _{CH₂, CH}	1.67-3	-0.219	-	-0.160	-	-0.152	-
H _{CHO}	3-4.5	0.741	0.003	0.650	0.009	0.452	0.047
H _{Ar}	6.0-8.25	0.786	0.002	0.608	0.013	0.843	0.001
H _{HCOO-}	8.29-8.45	0.838	0.001	0.617	0.012	0.648	0.009
H _{Ar} /H _{Al}							
H _{CHO} x H _{lAr}							
		0.883	<0.001	0.701	0.005	0.848	<0.001
		0.892	<0.001	0.739	0.003	0.745	0.003



Proposed binding sites for naturally occurring and laboratory iodination at ambient conc.



Functional group	Chemical structure	Proposed active aromatic ring for iodine binding*	^{13}C (ppm)	^1H (ppm)
$\text{C}_{\text{Alk}-\text{H,C}}$			160.2	7.17-7.36, 8.29
$\text{C}_{\text{Alk}-\text{O}}$			173.0	7.06-7.41
$\Sigma \text{C}_{\text{Alk}}$				
C_{Aro}				
$\text{C}_{\text{Ar-H,C}}$			185.2-188.2	7.17-7.65
$\text{C}_{\text{Ar-O}}$			171.4	7.08-7.58
$\Sigma \text{C}_{\text{Ar}}$				
C_{coo}				
$\text{C}_{\text{C=O}}$				
$\text{C}_{\text{Ar-H,C}}$	(108)			
$\times \text{C}_{\text{coo}}$	(108)			
$\times \text{C}^{\text{COO}}$	(108)		158.6	7.03-7.38
C_{Aro}				
$\Sigma \text{C}_{\text{Aro}}$				
$\text{C}_{\text{C=O}}$				

Kd	
R^2	p
.660	-
.152	-
452	0.047
843	0.001
648	0.009
848	0.000

36